REVISTA INTERDISCIPLINAR DE PESQUISA EM ENGENHARIA

CILAMCE 2016

XXXVII IBERIAN LATIN AMERICAN CONGRESS ON COMPUTATIONAL METHODS IN ENGINEERING
BRASÍLIA - DF - BRAZIL

UNSCENTED KALMAN FILTERS AND EXTENDED H_∞ FILTER FOR SPACECRAFT ATTITUDE ESTIMATION USING QUATERNIONS

William Reis Silva

reis.william@gmail.com

Division of Fundamental Sciences, Technological Institute of Aeronautics (ITA), CTA-ITA-IEFM

Pr. Marechal Eduardo Gomes, 50, Vila das Acácias, CEP: 12228-900 , São José dos Campos, São Paulo, Brazil.

Roberta Veloso Garcia

robertagarcia@usp.br

Lorena School of Engineering, São Paulo University (USP)

Estrada Municipal do Campinho, s/n, CEP: 12.602-810, Lorena, São Paulo, Brazil.

Hélio Koiti Kuga

helio.kuga@inpe.br

Space Mechanics and Control Division, National Institute for Space Research (INPE)

Av. dos Astronautas, 1758, Jardim da Granja, CEP: 12227-010, São José dos Campos, São Paulo, Brazil

Maria Cecília Zanardi

mceciliazanardi@gmail.com

Federal University of ABC (UFABC)

Av. dos Estados, 5001, Bangu, CEP:09210-580, Santo André, São Paulo, Brazil.

Abstract.

In this work, the attitude determination and the gyros drift estimation using the Uncented

Kalman Filter (UKF) and the Second-Order Extended H_∞ Filter (SOEH$_\infty$F) for nonlinear systems will be described. The extended H_∞ filter provides a rigorous method for dealing with systems that have model and noise uncertainties. Thus, extended H_∞ filter is simply a robust version of the extended Kalman filter because to add tolerance to unmodeled noise and dynamics. The Unscented Kalman Filter transforms a set of points (cloud) through known nonlinear equations and combines the results to estimate the mean and covariance of the state. The points (called sigma-points) are carefully selected on the basis of a specific criterion. The application uses the simulated measurement data for orbit and attitude of the CBERS-2 (China Brazil Earth Resources Satellite). The attitude model is described by quaternions and the attitude sensors available are two DSS (Digital Sun Sensors), two IRES (Infra-Red Earth Sensor), and one triad of mechanical gyros.The results in this work show that one can reach accuracies in attitude determination within the prescribed requirements, besides providing estimates of the gyro drifts which can be further used to enhance the gyro error model.

Keywords: *Unscented Kalman Filter, Extended H_∞ Filter, Attitude Estimation, Gyro Calibration, Nonlinear System*

1 INTRODUCTION

Attitude estimation is a process of determining the orientation of a satellite with respect to an inertial reference system by processing data from attitude sensors. Given a reference vector, the attitude sensor measures the orientation of this vector with respect to the satellite system. Then, it is possible to estimate the orientation of the satellite processing computationally these vectors using attitude estimation methods. The bias can be defined as a output component not related to input to which the sensor is subjected and its components have features deterministic and stochastic. Therefore, you need to know and to characterize it, consequently set the method for estimating.[1]

The attitude stabilization here is done in three axes namely geo-targeted, and can be described in relation to the orbital system. In this frame, the movement around the direction of the orbital speed is named *roll* (ϕ), the movement around the normal direction to the orbit is called *pitch* (θ), and finally the movement around the Zenith/Nadir direction is called *yaw* (ψ). See Figure 1.

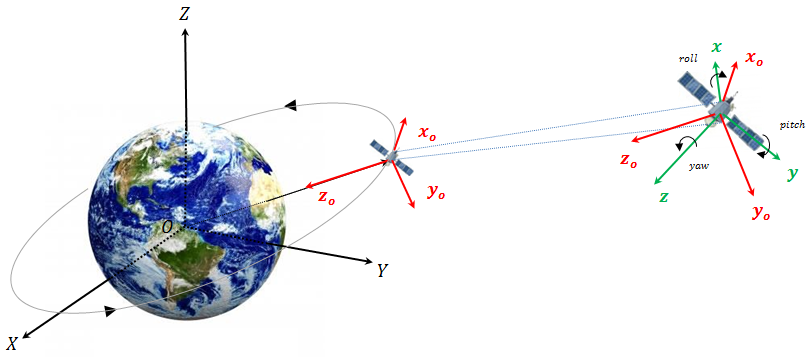

Figure 1: The orbital local system ($\mathbf{x}_o, \mathbf{y}_o, \mathbf{z}_o$) and the attitude system ($\mathbf{x}, \mathbf{y}, \mathbf{z}$)

In this work, the attitude model is described by quaternions and the contributions of this research is in the fact that, in the four estimation methods used, Second-Order Extended H_∞ Filter (SOEH_∞F), Extended H_∞ Filter (EH_∞F), Extended Kalman Filter (EKF) and the Unscented Kalman Filter (UKF) consider the process model as noisy, as noted in reality. Furthermore, the methods are considered online, which can be used on board the satellite, for each measurements processed, the methods propagates and updates the states estimated in real time.

In the simulation for orbit and attitude, performed by the propagator PROPAT,[2] again the sattelite considered has similar characteristics to CBERS-2 which have data supplied by triad of gyroscopes, two Infrared Earth Sensors (IRES) and two Digital Sun Sensors (DSS).

As previously mentioned, The state estimation process was performed by the SOEH_∞F compared to EH_∞F and EKF. Undoubtedly, the Kalman filter is most famous for its wide application in various areas of engineering. In Aerospace Engineering sector we can mention important contributions, the Reference[3] presents a study on the satellite attitude estimation using the Extended Kalman Filter, the Reference[4] presents comparisons between two Kalman Filters for nonlinear systems, the Reference[5] analyzes the results of the Extended Kalman Filter in instant mapping and localization process and in Reference,[6] research used as a model, because it uses

the Extended Kalman filter for attitude and gyros bias estimation but using real data and with a sampling time less than that used in this research.

The Kalman filtering assumes that the message generating process has a known dynamics and that the exogenous inputs have known statistical properties. Unfortunately, these assumptions limit the utility of minimum variance estimators in situations where the message model and the noise descriptions are unknown.[7]

Given this feature of Kalman filtering, is on this background that the H_∞ filtering used herein contributes to the better accuracy in the estimation process of spacecraft attitude.

The H_∞ filtering minimizes the worst-case estimation error and thus it is more robust than conventional Kalman filtering. The H_∞ Filter is based on the game theory approach that was originally developed by Reference[8] and is further discussed in Reference[9] and Reference.[10] The extended form for the H_∞ filtering with a second-order linearization is discussed in Reference.[11] In this game theory approach, the designer prepares for the worst strategy that the nature can provide. Therefore, the state estimator and the signal disturbance (initial condition error, process noise and measurements noise) have conflicting objectives, which are to mininize and maximize the estimation error respectively. The estimation criterion in the H_∞ filter design is to minimize the worst possible effects of the disturbance signals on the signal estimation error without *a priori* knowledge of them.

2 Attitude Representation by Quaternions

The quaternion is a four dimensional vector that defines a unit vector in space and the angle to rotate about that unit vector to transform from one frame to another.[12,13] The quaternion can be written as follows:

$$\boldsymbol{q} = \begin{bmatrix} q_1 & q_2 & q_3 & q_4 \end{bmatrix}^T = \begin{bmatrix} \boldsymbol{q}^* & q_4 \end{bmatrix}^T \tag{1}$$

where, $\boldsymbol{q}^* = \boldsymbol{e} \sin\dfrac{\zeta}{2}$ e $q_4 = \cos\dfrac{\zeta}{2}$

Here, $\boldsymbol{e} = \begin{bmatrix} e_1 & e_2 & e_3 \end{bmatrix}^T$ is the unit vector and ζ is the angle of rotation about unit vector $\boldsymbol{e}$. The quaternion satisfies the following constraint:

$$\boldsymbol{q}^T\boldsymbol{q} = q_1^2 + q_2^2 + q_3^2 + q_4^2 = 1 \tag{2}$$

The state vector formed by the quaternion and the gyro bias vector is given by:

$$\boldsymbol{x} = \begin{bmatrix} q_1 & q_2 & q_3 & q_4 & \varepsilon_x & \varepsilon_y & \varepsilon_z \end{bmatrix}^T \tag{3}$$

If the angular velocity vector $\boldsymbol{\omega} = \begin{bmatrix} \omega_x & \omega_y & \omega_z \end{bmatrix}^T$ of body frame is known with respect to another reference frame, the differential equation of the quaternion system becomes[3,12]

$$\begin{aligned} \dot{\boldsymbol{q}} &= \frac{1}{2}\boldsymbol{\Omega}_\omega \boldsymbol{q} \\ \dot{\boldsymbol{\varepsilon}} &= 0 \end{aligned} \tag{4}$$

where, $\mathbf{\Omega}_\omega$ is an anti-symmetric matrix 4×4 given by:

$$\mathbf{\Omega}_\omega = \begin{bmatrix} 0 & \omega_z & -\omega_y & \omega_x \\ -\omega_z & 0 & \omega_x & \omega_y \\ \omega_y & -\omega_x & 0 & \omega_z \\ -\omega_x & -\omega_y & -\omega_z & 0 \end{bmatrix} \tag{5}$$

Assuming that the working data is sampled at a fixed rate and the angular velocity vector in the satellite system is constant over the sampling interval, then a solution of the problem is:[13]

$$\boldsymbol{q}\left(t_{k+1}\right) = \mathbf{\Phi}_{\boldsymbol{q}}\left(\Delta t, |\boldsymbol{\omega}|\right) \boldsymbol{q}\left(t_k\right) \tag{6}$$

where, Δt the sampling interval; $\boldsymbol{q}\left(t_k\right)$ is the attitude quaternion in time t_k; $\boldsymbol{q}\left(t_{k+1}\right)$ is the quaternion of propagated attitude to time t_{k+1}; and $\mathbf{\Phi}_{\boldsymbol{q}}$ is the transition matrix carrying the system time t_{k+1} for t_k , given by:

$$\mathbf{\Phi}_{\boldsymbol{q}}\left(\Delta t, |\boldsymbol{\omega}|\right) = \cos\left(\frac{|\boldsymbol{\omega}|\,\Delta t}{2}\right)\boldsymbol{I} + \frac{1}{|\boldsymbol{\omega}|}\sin\left(\frac{|\boldsymbol{\omega}|\,\Delta t}{2}\right)\mathbf{\Omega}_\omega \tag{7}$$

3 Mathematical Models of Attitude Sensors

In order to ascertain the attitude of an artificial satellite it is necessary to use some attitude sensors. Thus, in this section is described the mathematical model of the attitude sensors used in this research for the determination of attitude: gyros, digital sun sensor and infrared Earth sensor.

3.1 Mathematical Model of Gyroscope

In this work the gyros (*Rate Integration Gyros-RIG's*) are used to measure the angular velocity of roll, pitch and yaw axes of the satellite. In addition, the drift errors (bias), due to minor imperfections of its mechanism, are included in the state vector to be estimated.

The bias can be defined as an output component not related to input to which the sensor is subjected and its components have features deterministic and stochastic. Therefore, you need to characterize it and consequently set the method for estimating.

The RIG's model is given by:[13]

$$\Delta\mathbf{\Theta}_i = \int_0^{\Delta t} \left(\boldsymbol{\omega}_i + \boldsymbol{\varepsilon}_i\right) dt, \qquad (i = x, y, z) \tag{8}$$

where, $\Delta\mathbf{\Theta}_i$ are the angular displacements measured in the axes of the satellite in a time interval Δt, $\boldsymbol{\omega}_i$ are the components of the angular velocity of the satellite system and $\boldsymbol{\varepsilon}_i$ are the components of the gyro bias.

The measurement of the components of the angular velocity of the satellite is represented as:

$$\hat{\boldsymbol{\omega}}_i = \frac{d\mathbf{\Theta}_i}{dt} - \hat{\boldsymbol{\varepsilon}}_i - \boldsymbol{\eta}_i = \boldsymbol{g}_i - \hat{\boldsymbol{\varepsilon}}_i + \boldsymbol{\upsilon}_i \tag{9}$$

where, $\boldsymbol{g}_i(t)$ is the gyro output vector and $\boldsymbol{\upsilon}_i(t)$ is the white Gaussian noise process, which covers all remaining non-modeled effects besides the random noises.

3.2 Mathematical Model of Infrared Earth Sensor

The horizon Sensor is an optical instrument used to detect the light emitted by the edge of the Earth's atmosphere. Infrared sensors are used to detect the heat from the Earth's atmosphere, which is very hot compared to the cold of space, thus they are called Infrared Earth Sensors(IRES). The IRES determine the angle between the direction of an axis of symmetry of the satellite and the direction from the center of the Earth.

When using the IRES, it may help to estimate drift errors present in gyro.[3,14] In this work, two sensors are used, where one measures the *roll* angle and the other measures the *pitch* angle.

The equations of measurements for Infrared Earth Sensors (IRES) are given by.[15]

$$\begin{aligned} \phi_H &= \phi + \upsilon_{\phi_H} \\ \theta_H &= \theta + \upsilon_{\theta_H} \end{aligned} \tag{10}$$

where υ_{ϕ_H} and υ_{θ_H} are the white noise that represent small remaining effects of misalignment during installation and/or by assembly of sensor. These errors are assumed Gaussian ones.

3.3 Mathematical Model of Digital Sun Sensor

The Digital Sun Sensor is an optical device that detects the Sun and sets the position of one of the main axes of symmetry of the spacecraft relative to the direction in which the Sun was detected. In this work is not able to measure the *yaw* angle, *i.e.*, these sensors do not provide direct measures, it measures the coupled *pitch* angle (α_θ) and *yaw* angle (α_ψ). The equations of measurements for the Digital Sun Sensors (DSS) are obtained as follows.[15–17]

$$\alpha_\psi = \arctan\left(\frac{-S_y}{S_x\cos 60^\circ + S_z\cos 150^\circ}\right) + \upsilon_{\alpha_\psi} \tag{11}$$

when $|S_x\cos 60^\circ + S_z\cos 150^\circ| \geq \cos 60^\circ$, and

$$\alpha_\theta = 24^\circ + \arctan\left(\frac{S_x}{S_z}\right) + \upsilon_{\alpha_\theta} \tag{12}$$

when $\left|24^\circ + \arctan\left(\frac{S_x}{S_z}\right)\right| < 60^\circ$, where υ_{α_ψ} and υ_{α_θ} are the white noise and represent small effects remnants of misalignment during installation and/or by sensor assembly. Just as the Infrared Earth Sensor, these errors are assumed Gaussian ones.

The conditions must be such that the solar vector is in the field of sight of sensor and S_x, S_y, S_z are the components of the unit vector associated with the solar vector satellite system at date by:

$$\begin{aligned} S_x &= S_{0x} + \psi S_{0y} - \theta S_{0z} \\ S_y &= S_{0y} - \psi S_{0x} + \phi S_{0z} \\ S_z &= S_{0z} - \phi S_{0y} - \theta S_{0z} \end{aligned} \tag{13}$$

where S_{0x}, S_{0y} e S_{0z} are the components of the solar vector in orbital coordinate system[15] and ϕ, θ e ψ are the Euler angles, which represent the estimated attitude.

4 Problem Formulation for the Second-Order Extended H_∞ Filter

Consider a nonlinear discrete time system

$$\begin{aligned} \boldsymbol{x}_{k+1} &= f(\boldsymbol{x}_k, \boldsymbol{u}_k) + \boldsymbol{w}_k \\ \boldsymbol{y}_k &= h(\boldsymbol{x}_k) + \boldsymbol{v}_k \end{aligned} \tag{14}$$

where k is the discrete time index, $\boldsymbol{x}_{k+1}$ and $\boldsymbol{y}_k$ are the state and measurements vectors with dimensions of n and m respectively, $\boldsymbol{w}_k$ and $\boldsymbol{v}_k$ are process and measurements noises, these noise terms may be random with possibly unknown statistics and nonzero mean, or they may be deterministic. The term $\boldsymbol{u}_k$ is the control input and $f(.)$ and $h(.)$ are vectors of nonlinear functions that are differentiable with respect to $\boldsymbol{x}_k$.

Hence, the second-order Taylor series expansion of $f(\boldsymbol{x}_k, \boldsymbol{u}_k)$ and $h(\boldsymbol{x}_k)$ around the nominal point $\hat{\boldsymbol{x}}_k$ (the estimated state) are

$$\begin{aligned} f(\boldsymbol{x}_k, \boldsymbol{u}_k) &= f(\hat{\boldsymbol{x}}_k, \boldsymbol{u}_k) + \left.\frac{\partial f}{\partial \boldsymbol{x}_k}\right|_{\hat{\boldsymbol{x}}_k} (\boldsymbol{x}_k - \hat{\boldsymbol{x}}_k) \\ &\quad + \frac{1}{2}\sum_{i=1}^{n} \varphi_i^f \, (\boldsymbol{x}_k - \hat{\boldsymbol{x}}_k)^T \left.\frac{\partial^2 f_i}{\partial \boldsymbol{x}_k^2}\right|_{\hat{\boldsymbol{x}}_k} (\boldsymbol{x}_k - \hat{\boldsymbol{x}}_k) \end{aligned} \tag{15}$$

$$\begin{aligned} h(\boldsymbol{x}_k) &= h(\hat{\boldsymbol{x}}_k) + \left.\frac{\partial h}{\partial \boldsymbol{x}_k}\right|_{\hat{\boldsymbol{x}}_k} (\boldsymbol{x}_k - \hat{\boldsymbol{x}}_k) \\ &\quad + \frac{1}{2}\sum_{i=1}^{m} \varphi_i^h \, (\boldsymbol{x}_k - \hat{\boldsymbol{x}}_k)^T \left.\frac{\partial^2 h_i}{\partial \boldsymbol{x}_k^2}\right|_{\hat{\boldsymbol{x}}_k} (\boldsymbol{x}_k - \hat{\boldsymbol{x}}_k) \end{aligned} \tag{16}$$

where f_i and h_i are the ith element of $f(\boldsymbol{x}_k, \boldsymbol{u}_k)$ and $h(\boldsymbol{x}_k)$. The terms φ_i^f and φ_i^h are vectors given by $\varphi_i^f = \begin{bmatrix} 0 & ... & 0 & 1 & 0 & ... & 0 \end{bmatrix}^T_{n\times 1}$ and $\varphi_i^h = \begin{bmatrix} 0 & ... & 0 & 1 & 0 & ... & 0 \end{bmatrix}^T_{m\times 1}$ where the one is in the ith element. The quadratic term in Eq. (15) and (16) can be written as

$$\begin{aligned} (\boldsymbol{x}_k - \hat{\boldsymbol{x}}_k)^T \left.\frac{\partial^2 f_i}{\partial \boldsymbol{x}_k^2}\right|_{\hat{\boldsymbol{x}}_k} (\boldsymbol{x}_k - \hat{\boldsymbol{x}}_k) &= tr\left[\left.\frac{\partial^2 f_i}{\partial \boldsymbol{x}_k^2}\right|_{\hat{\boldsymbol{x}}_k} (\boldsymbol{x}_k - \hat{\boldsymbol{x}}_k)(\boldsymbol{x}_k - \hat{\boldsymbol{x}}_k)^T\right] \\ &\approx tr\left[\left.\frac{\partial^2 f_i}{\partial \boldsymbol{x}_k^2}\right|_{\hat{\boldsymbol{x}}_k} \bar{\boldsymbol{P}}_k\right] \end{aligned} \tag{17}$$

$$\begin{aligned} (\boldsymbol{x}_k - \hat{\boldsymbol{x}}_k)^T \left.\frac{\partial^2 h_i}{\partial \boldsymbol{x}_k^2}\right|_{\hat{\boldsymbol{x}}_k} (\boldsymbol{x}_k - \hat{\boldsymbol{x}}_k) &= tr\left[\left.\frac{\partial^2 h_i}{\partial \boldsymbol{x}_k^2}\right|_{\hat{\boldsymbol{x}}_k} (\boldsymbol{x}_k - \hat{\boldsymbol{x}}_k)(\boldsymbol{x}_k - \hat{\boldsymbol{x}}_k)^T\right] \\ &\approx tr\left[\left.\frac{\partial^2 h_i}{\partial \boldsymbol{x}_k^2}\right|_{\hat{\boldsymbol{x}}_k} \bar{\boldsymbol{P}}_k\right] \end{aligned} \tag{18}$$

where $tr\,[.]$ is the trace operation and it was assumed that the matrix $\bar{\boldsymbol{P}}_k$ can be estimated by the sample covariance matrix of the estimation error.

The goal is to estimate a linear combination of the state. That is, we want to estimate $\boldsymbol{z}_k$, which is given by

$$\boldsymbol{z}_k = \boldsymbol{L}_k \boldsymbol{x}_k \tag{19}$$

where $\boldsymbol{L}_k$ is a user-defined matrix with full rank. If we want to directly estimate $\boldsymbol{x}_k$ as in the Kalman Filter, then we set $\boldsymbol{L}_k = \boldsymbol{I}$. The estimate of $\boldsymbol{z}_k$ is denoted as $\hat{\boldsymbol{z}}_k$ and the estimate of the initial state $\boldsymbol{x}_0$ is $\hat{\boldsymbol{x}}_0$.

The design criterion for the SOEH_∞F is to find $\hat{\boldsymbol{z}}_k$ that minimizes $(\boldsymbol{z}_k - \hat{\boldsymbol{z}}_k)$ for any $\boldsymbol{w}_k$, $\boldsymbol{v}_k$ and $\boldsymbol{x}_0$. Considering the worst-case scenario, assuming that the nature is our adversary one needs to find $\boldsymbol{w}_k$, $\boldsymbol{v}_k$ and $\boldsymbol{x}_0$ to maximize $(\boldsymbol{z}_k - \hat{\boldsymbol{z}}_k)$.[11,18]

However, the nature could maximize $(z_k - \hat{z}_k)$ by simply using infinite magnitudes for $\boldsymbol{w}_k$, $\boldsymbol{v}_k$ and $\boldsymbol{x}_0$, but this would not make the game fair, as this is not a clever choice. One of the ideas is to put the terms $\boldsymbol{w}_k$, $\boldsymbol{v}_k$ and $\boldsymbol{x}_0$ in the denominator and a commonly used cost function is

$$J_1 = \frac{\displaystyle\sum_{k=0}^{N-1} \|\boldsymbol{z}_k - \hat{\boldsymbol{z}}_k\|^2_{\boldsymbol{S}_k}}{\|\boldsymbol{x}_0 - \hat{\boldsymbol{x}}_0\|^2_{\boldsymbol{P}_0^{-1}} + \displaystyle\sum_{k=0}^{N-1} \left(\|\boldsymbol{w}_k\|^2_{\boldsymbol{Q}_k^{-1}} + \|\boldsymbol{v}_k\|^2_{\boldsymbol{R}_k^{-1}} \right)} \tag{20}$$

The notation $\|\boldsymbol{x}_k\|^2_{\boldsymbol{S}_k}$ is defined as the square of the $\boldsymbol{x}_k$ weighted by $\boldsymbol{S}_k$, or the L_2 norm of $\boldsymbol{x}_k$, *i.e.*, $\|\boldsymbol{x}_k\|^2_{\boldsymbol{S}_k} = \boldsymbol{x}_k^T \boldsymbol{S}_k \boldsymbol{x}_k$. The weighting matrices $\boldsymbol{P}_0$, $\boldsymbol{Q}_k$, $\boldsymbol{R}_k$ and $\boldsymbol{S}_k$ are symmetric positive definite matrices chosen by the user based on the specific problem.

To solve of the minimax problem, first a stationary point of J_1 with respect to $\boldsymbol{x}_0$ and $\boldsymbol{w}_k$ needs to be found, and then a stationary point of J with respect to $\hat{\boldsymbol{x}}_k$ and $\boldsymbol{y}_k$ needs to be found too.[18]

4.1 The Second-Order Extended H_∞ Filter Solution

Consider the minimax problem, the Taylor series expansion described in Eq. (15) and (16) is used to approximate the nonlinear function in Eq. (14). The stationary point of J_1 with respect to $\boldsymbol{x}_0$ and $\boldsymbol{w}_k$ is given by

$$\boldsymbol{x}_0 = \hat{\boldsymbol{x}}_0 + \boldsymbol{P}_0 \boldsymbol{\lambda}_0 \tag{21}$$

$$\boldsymbol{w}_k = \boldsymbol{Q}_k \boldsymbol{\lambda}_{k+1} \tag{22}$$

$$\boldsymbol{\lambda}_N = 0 \tag{23}$$

$$\boldsymbol{\lambda}_k = \boldsymbol{G}_k^{-1} \left[\boldsymbol{F}_k^T \boldsymbol{\lambda}_{k+1} + \gamma \bar{\boldsymbol{S}}_k \left(\boldsymbol{\mu}_k - \hat{\boldsymbol{x}}_k \right) + \boldsymbol{H}_k^T \boldsymbol{R}_k^{-1} \left(\tilde{\boldsymbol{y}}_k - \boldsymbol{H}_k \left(\boldsymbol{\mu}_k - \hat{\boldsymbol{x}}_k \right) \right) \right] \tag{24}$$

$$\boldsymbol{P}_{k+1} = \boldsymbol{F}_k \boldsymbol{P}_k \boldsymbol{G}_k^{-1} \boldsymbol{F}_k^T + \boldsymbol{Q}_k \tag{25}$$

$$\boldsymbol{\mu}_0 = \hat{\boldsymbol{x}}_0 \tag{26}$$

$$\begin{aligned} \boldsymbol{\mu}_{k+1} \;=\; & f\left(\hat{\boldsymbol{x}}_k, \boldsymbol{\mu}_k\right) + \boldsymbol{F}_k \left(\boldsymbol{\mu}_k - \hat{\boldsymbol{x}}_k \right) + \frac{1}{2} \sum_{i=1}^{n} \varphi_i^f tr \left[\left. \frac{\partial^2 f_i}{\partial \boldsymbol{x}_k^2} \right|_{\hat{\boldsymbol{x}}_k} \bar{\boldsymbol{P}}_k \right] \\ & + \boldsymbol{F}_k \boldsymbol{P}_k \boldsymbol{G}_k^{-1} \left[\gamma \bar{\boldsymbol{S}}_k \left(\boldsymbol{\mu}_k - \hat{\boldsymbol{x}}_k \right) + \boldsymbol{H}_k^T \boldsymbol{R}_k^{-1} \left(\tilde{\boldsymbol{y}}_k - \boldsymbol{H}_k \left(\boldsymbol{\mu}_k - \hat{\boldsymbol{x}}_k \right) \right) \right] \end{aligned} \tag{27}$$

where

$$\boldsymbol{F}_k = \left.\frac{\partial f}{\partial \boldsymbol{x}_k}\right|_{\hat{\boldsymbol{x}}_k} \tag{28}$$

$$\boldsymbol{H}_k = \left.\frac{\partial h}{\partial \boldsymbol{x}_k}\right|_{\hat{\boldsymbol{x}}_k} \tag{29}$$

$$\tilde{\boldsymbol{y}}_k = \boldsymbol{y}_k - h\left(\hat{\boldsymbol{x}}_k\right) - \frac{1}{2}\sum_{i=1}^{m} \varphi_i^h tr\left[\left.\frac{\partial^2 h_i}{\partial \boldsymbol{x}_k^2}\right|_{\hat{\boldsymbol{x}}_k} \bar{\boldsymbol{P}}_k\right] \tag{30}$$

$$\boldsymbol{G}_k = \boldsymbol{I} - \gamma \bar{\boldsymbol{S}}_k \boldsymbol{P}_k + \boldsymbol{H}_k^T \boldsymbol{R}_k^{-1} \boldsymbol{H}_k \boldsymbol{P}_k \tag{31}$$

The Eq. (30) is called residual and its has fundamental importance for the stability and convergence of the filter.

With the results of $\boldsymbol{x}_0$ and $\boldsymbol{w}_k$ present in Eq. (21) and (22), the stationary point of J with respect to $\hat{\boldsymbol{x}}_k$ and $\boldsymbol{y}_k$ is given by

$$\hat{\boldsymbol{x}}_k = \boldsymbol{\mu}_k \tag{32}$$

$$\boldsymbol{y}_k = h\left(\hat{\boldsymbol{x}}_k\right) + \frac{1}{2}\sum_{i=1}^{m} \varphi_i^h tr\left[\left.\frac{\partial^2 h_i}{\partial \boldsymbol{x}_k^2}\right|_{\boldsymbol{x}_k} \bar{\boldsymbol{P}}_k\right] \tag{33}$$

The proof and the mathematical development can be found in Reference[11] and Reference.[18]

However, the SOEH_∞F Solution, presented for the space state represented by Eq. (14), is given by combination of the Eq. (27), (25), (32) and (33), thus:[11,18]

$$\bar{\boldsymbol{S}}_k = \boldsymbol{L}_k^T \boldsymbol{S}_k \boldsymbol{L}_k \tag{34}$$

$$\boldsymbol{K}_k = \boldsymbol{P}_k \left[\boldsymbol{I} - \gamma \bar{\boldsymbol{S}}_k \boldsymbol{P}_k + \boldsymbol{H}_k^T \boldsymbol{R}_k^{-1} \boldsymbol{H}_k \boldsymbol{P}_k\right]^{-1} \boldsymbol{H}_k^T \boldsymbol{R}_k^{-1} \tag{35}$$

$$\hat{\boldsymbol{x}}_{k+1} = f(\hat{\boldsymbol{x}}_k, \boldsymbol{\mu}_k) + \frac{1}{2}\sum_{i=1}^{n} \varphi_i^f tr\left[\left.\frac{\partial^2 f_i}{\partial \boldsymbol{x}_k^2}\right|_{\hat{\boldsymbol{x}}_k} \bar{\boldsymbol{P}}_k\right] + \boldsymbol{F}_k \boldsymbol{K}_k \tilde{\boldsymbol{y}}_k \tag{36}$$

$$\boldsymbol{P}_{k+1} = \boldsymbol{F}_k \boldsymbol{P}_k \left[\boldsymbol{I} - \gamma \bar{\boldsymbol{S}}_k \boldsymbol{P}_k + \boldsymbol{H}_k^T \boldsymbol{R}_k^{-1} \boldsymbol{H}_k \boldsymbol{P}_k\right]^{-1} \boldsymbol{F}_k^T + \boldsymbol{Q}_k \tag{37}$$

$$\boldsymbol{\lambda}_{k+1} = \left(\boldsymbol{F}_k \boldsymbol{F}_k^T + \xi \boldsymbol{I}\right)^{-1} \boldsymbol{F}_k \left(\boldsymbol{G}_k \boldsymbol{\lambda}_k - \boldsymbol{H}_k^T \boldsymbol{R}_k^{-1} \tilde{\boldsymbol{y}}_k\right) \tag{38}$$

$$\bar{\boldsymbol{P}}_{k+1} = \eta \bar{\boldsymbol{P}}_k + (1-\eta)\, \boldsymbol{P}_k \boldsymbol{\lambda}_k \boldsymbol{\lambda}_k^T \boldsymbol{P}_k^T \tag{39}$$

where ξ is positive scalar to prevent the term $\boldsymbol{F}_k \boldsymbol{F}_k^T$ from being singular and $0 < \eta \leq 1$. Furthermore, the value of γ must satisfy the Eq. (40) to ensure that the optimized value of $\hat{\boldsymbol{x}}_k$ yields a local minimum of J, *i.e.*

$$\boldsymbol{P}_k^{-1} - \gamma \bar{\boldsymbol{S}}_k + \boldsymbol{H}_k^T \boldsymbol{R}_k^{-1} \boldsymbol{H}_k > 0 \tag{40}$$

That is, the expression, $\boldsymbol{P}_k^{-1} - \gamma \bar{\boldsymbol{S}}_k + \boldsymbol{H}_k^T \boldsymbol{R}_k^{-1} \boldsymbol{H}_k$, must be positive definite.

4.2 The Extended H_∞ Filter Solution

The Solution is similar to presented in SOEH_∞F Solution but without the second order terms.[19]

However, the EH_∞F Solution is given by:

$$\bar{\boldsymbol{S}}_k = \boldsymbol{L}_k^T \boldsymbol{S}_k \boldsymbol{L}_k \tag{41}$$

$$\boldsymbol{K}_k = \boldsymbol{P}_k \left[\boldsymbol{I} - \gamma \bar{\boldsymbol{S}}_k \boldsymbol{P}_k + \boldsymbol{H}_k^T \boldsymbol{R}_k^{-1} \boldsymbol{H}_k \boldsymbol{P}_k\right]^{-1} \boldsymbol{H}_k^T \boldsymbol{R}_k^{-1} \tag{42}$$

$$\hat{\boldsymbol{x}}_{k+1} = f(\hat{\boldsymbol{x}}_k, \boldsymbol{\mu}_k) + \boldsymbol{F}_k \boldsymbol{K}_k \left(\boldsymbol{y}_k - h\left(\hat{\boldsymbol{x}}_k\right)\right) \tag{43}$$

$$\boldsymbol{P}_{k+1} = \boldsymbol{F}_k \boldsymbol{P}_k \left[\boldsymbol{I} - \gamma \bar{\boldsymbol{S}}_k \boldsymbol{P}_k + \boldsymbol{H}_k^T \boldsymbol{R}_k^{-1} \boldsymbol{H}_k \boldsymbol{P}_k\right]^{-1} \boldsymbol{F}_k^T + \boldsymbol{Q}_k \tag{44}$$

Again, the value of γ must satisfy the Eq. (44) to ensure that the optimized value of $\hat{\boldsymbol{x}}_k$ yields a local minimum of J, as was shown in Eq. (40)

4.3 The Extended Kalman Filter Solution

The EKF Solution for the nonlinear function, present in Eq. (14), is given as follows.[18]

Time update equations:

$$\hat{\boldsymbol{x}}_k^- = f(\hat{\boldsymbol{x}}_{k-1}^+, \boldsymbol{\mu}_k) \tag{45}$$

$$\tilde{\boldsymbol{P}}_k^- = \tilde{\boldsymbol{F}}_{k-1} \tilde{\boldsymbol{P}}_{k-1}^+ \tilde{\boldsymbol{F}}_{k-1}^T + \tilde{\boldsymbol{Q}}_{k-1} \tag{46}$$

Measurements update equations:

$$\hat{\boldsymbol{x}}_k^+ = \hat{\boldsymbol{x}}_k^- + \tilde{\boldsymbol{K}}_k \left(\boldsymbol{y}_k - h(\hat{\boldsymbol{x}}_k^-)\right) \tag{47}$$

$$\tilde{\boldsymbol{K}}_k = \tilde{\boldsymbol{P}}_k^- \tilde{\boldsymbol{H}}_k^T \left(\tilde{\boldsymbol{H}}_k \tilde{\boldsymbol{P}}_k^- \tilde{\boldsymbol{H}}_k^T + \tilde{\boldsymbol{R}}_k\right)^{-1} \tag{48}$$

$$\tilde{\boldsymbol{P}}_k^+ = \left(\boldsymbol{I} - \tilde{\boldsymbol{K}}_k \tilde{\boldsymbol{H}}_k\right) \tilde{\boldsymbol{P}}_k^- \tag{49}$$

where $\tilde{\boldsymbol{F}}_k = \left.\frac{\partial f}{\partial \boldsymbol{x}_k}\right|_{\hat{\boldsymbol{x}}_k^+}$ and $\tilde{\boldsymbol{H}}_k = \left.\frac{\partial h}{\partial \boldsymbol{x}_k}\right|_{\hat{\boldsymbol{x}}_k^-}$.

5 The Unscented Kalman Filter

The method calculates the statistics of a random variable that passes through a nonlinear transformation is called Unscented Transformation . This transformation is based on the principle that it is easier to approximate a probability distribution than approaching a nonlinear arbitrary function[18,20]

5.1 The Unscented Kalman Filter Solution

Consider the nonlinear function, present in Eq. (14) and n the number of state. Propagate it should be a time step $(k-1)$ to k, you must first choose the sigma-points $\boldsymbol{x}_{k-1}^{(i)}$, since the current best guess for the mean and covariance of $\boldsymbol{x}_k$ are $\boldsymbol{x}_{k-1}^{+}$ and $\boldsymbol{P}_{k-1}^{+}$:

$$\begin{aligned} \boldsymbol{x}^{(0)} &= \boldsymbol{x}_{k-1}^{+} \\ \boldsymbol{x}_{k-1}^{(i)} &= \boldsymbol{x}_{k-1}^{+} + \tilde{\boldsymbol{x}}^{(i)} \qquad i = 1, \ldots, 2n \\ \tilde{\boldsymbol{x}}^{(i)} &= \left(\sqrt{(n+\kappa)\,\boldsymbol{P}_{k-1}^{+}}\right)_i^T \qquad i = 1, \ldots, n \\ \tilde{\boldsymbol{x}}^{(n+i)} &= -\left(\sqrt{(n+\kappa)\,\boldsymbol{P}_{k-1}^{+}}\right)_i^T \qquad i = 1, \ldots, n \end{aligned} \tag{50}$$

Use the known equation of the nonlinear system $f(.)$ to convert the sigma-points $\boldsymbol{x}_k^{(i)}$ in vectors:

$$\hat{\boldsymbol{x}}_k^{(i)} = f(\hat{\boldsymbol{x}}_{k-1}^{(i)}, t_k) \qquad i = 0, \ldots, 2n \tag{51}$$

Combine the vector $\hat{\boldsymbol{x}}_k^{(i)}$ for the *a-priori* state estimated time k.

$$\hat{\boldsymbol{x}}_k^{-} = \sum_{i=0}^{2n} \boldsymbol{W}^{(i)} \hat{\boldsymbol{x}}_k^{(i)} \tag{52}$$

Estimate the *a-priori* error covariance. However, should add $\boldsymbol{Q}_{k-1}$ in the end of the process equation to take the noise in consideration:

$$\boldsymbol{P}_k^{-} = \sum_{i=0}^{2n} \boldsymbol{W}^{(i)} \left(\hat{\boldsymbol{x}}_k^{(i)} - \hat{\boldsymbol{x}}_k^{-}\right) \left(\hat{\boldsymbol{x}}_k^{(i)} - \hat{\boldsymbol{x}}_k^{-}\right)^T + \boldsymbol{Q}_{k-1} \tag{53}$$

Choose the sigma-points $\hat{\boldsymbol{x}}_k^{(i)}$, with appropriate changes to the mean and covariance of $\boldsymbol{x}_k$ are $\hat{\boldsymbol{x}}_k^{-}$ and $\hat{\boldsymbol{P}}_k^{-}$:

$$\begin{aligned} \boldsymbol{x}^{(0)} &= \boldsymbol{x}_k^{-} \\ \boldsymbol{x}_k^{(i)} &= \boldsymbol{x}_k^{-} + \tilde{\boldsymbol{x}}^{(i)} \qquad i = 1, \ldots, 2n \\ \tilde{\boldsymbol{x}}^{(i)} &= \left(\sqrt{(n+\kappa)\,\boldsymbol{P}_k^{-}}\right)_i^T \qquad i = 1, \ldots, n \\ \tilde{\boldsymbol{x}}^{(n+i)} &= -\left(\sqrt{(n+\kappa)\,\boldsymbol{P}_k^{-}}\right)_i^T \qquad i = 1, \ldots, n \end{aligned} \tag{54}$$

Use known nonlinear measurement equation $h(.)$ to convert the sigma-points in vectors $\hat{\boldsymbol{y}}_k^{(i)}$ (predicted measurement):

$$\hat{\boldsymbol{y}}_k^{(i)} = h(\hat{\boldsymbol{x}}_k^{(i)}, t_k) \qquad i = 0, \ldots, 2n \tag{55}$$

Combine the vector $\hat{\boldsymbol{y}}_k^{(i)}$ for the predicted measurement in time k

$$\hat{\boldsymbol{y}}_k = \sum_{i=0}^{2n} \boldsymbol{W}^{(i)} \hat{\boldsymbol{y}}_k^{(i)} \tag{56}$$

Estimate the covariance of the predicted measurements. However, should add $\boldsymbol{R}_k$ to the end of the equation to the take the measurement noise into account:

$$\boldsymbol{P}_y = \sum_{i=0}^{2n} \boldsymbol{W}^{(i)} \left(\hat{\boldsymbol{y}}_k^{(i)} - \hat{\boldsymbol{y}}_k\right) \left(\hat{\boldsymbol{y}}_k^{(i)} - \hat{\boldsymbol{y}}_k\right)^T + \boldsymbol{R}_k \tag{57}$$

Estimate the cross covariance between $\hat{\boldsymbol{x}}_k^-$ and $\hat{\boldsymbol{y}}_k$:

$$\boldsymbol{P}_{xy} = \sum_{i=0}^{2n} \boldsymbol{W}^{(i)} \left(\hat{\boldsymbol{x}}_k^{(i)} - \hat{\boldsymbol{x}}_k^-\right) \left(\hat{\boldsymbol{y}}_k^{(i)} - \hat{\boldsymbol{y}}_k\right)^T \tag{58}$$

The updated measures of estimated state can be obtained using the Kalman filter Normal as follows:

$$\begin{aligned} \boldsymbol{K}_k &= \boldsymbol{P}_{xy} \boldsymbol{P}_y^{-1} \\ \hat{\boldsymbol{x}}_k^+ &= \hat{\boldsymbol{x}}_k^- + \boldsymbol{K}_k \left(\boldsymbol{y}_k - \hat{\boldsymbol{y}}_k\right) \\ \boldsymbol{P}_k^+ &= \boldsymbol{P}_k^- - \boldsymbol{K}_k \boldsymbol{P}_y \boldsymbol{K}_k^T \end{aligned} \tag{59}$$

6 Computer Simulation by PROPAT and Results

The orbit and attitude simulation were made by propagator PROPAT,[2] coded in MatLab software with a sampling rate of $0.5s$ for $10min$ of observation.

The initial conditions used were $\boldsymbol{x}_0 = \begin{bmatrix} 0.0 & 0.0 & 0.0 & 5.76 & 4.83 & 2.68 \end{bmatrix}^T$; the covariance matrix $\boldsymbol{P}_0 = diag\left(0.25; 0.25; 4.0; 1.0; 1.0; 1.0\right)$; the process error matrix which weigh the process noise $\boldsymbol{Q}_0 = diag\left(6.08; 5.47; 6.08; 4 \times 10^{-3}; 4 \times 10^{-3}; 4 \times 10^{-3}\right) \times 10^{-3}$; the measurements error matrix which weigh the measurements noise $\boldsymbol{R}_0 = diag\left(0.36; 0.36; 0.0036; 0.0036\right)$; the auxiliar covariance matrix $\bar{\boldsymbol{P}}_0 = diag\left(0.25; 0.25; 4.0; 1.0; 1.0; 1.0\right)$ and the initial Lagrange multiplier $\boldsymbol{\lambda}_0 = \begin{bmatrix} 0.1 & 0.1 & 0.1 & 0.1 & 0.1 & 0.1 \end{bmatrix}^T$. For the vector $\boldsymbol{x}_0$, the first three elements are in deg and the others elements are in deg/h, for the matrices $\boldsymbol{P}_0$, $\boldsymbol{Q}_0$ and $\bar{\boldsymbol{P}}_0$ the first three elements are in deg^2 and the others elements are in deg^2/h^2, and finally, for the matrix $\boldsymbol{R}_0$ all the elements are in deg^2.

For the SOEH_∞F, the parameters used were $\gamma = 1/3$, $\eta = 0.01$, $\xi = 10.3$ and the matrices $\boldsymbol{L}_k$ and $\boldsymbol{S}_k$ are both set to be identity matrices.

Figures 2 and 3, present the attitude angles and gyros bias estimation using the EKF, EH_∞F, SOEH_∞F and the UKF.

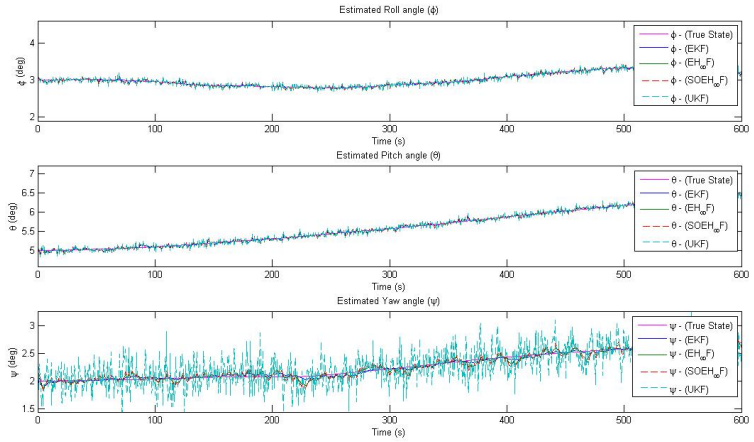

Figure 2: Estimated *roll*, *pitch* and *yaw* angles respectively

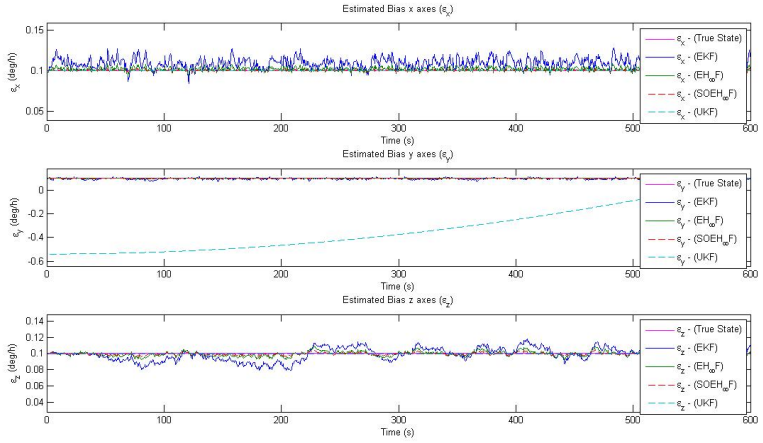

Figure 3: Estimated gyros bias around the x, y and z axes respectively

Figure 2 can be see that for the *roll* and *pitch* angles of both filters are consistent, but for the *yaw* angle is observed that the UKF has a more oscillating result which leads us to consider the SOEH_∞F with better result for the respective estimated angle. In Fig. 3, it is observed that the UKF has a higher accuracy for the gyros bias around the **x** and **z** axes, but for the gyros bias around the **y** axes the UKF delay to converge, thus the SOEH_∞F presents greater accuracy for the gyros bias around the **y**.

It is importante to emphasize that the Kalman Filter can be made more robust to noise and dynamics unmodeled by artificially increasing the process noise covariance matrix $\tilde{\boldsymbol{Q}}_k$ which results in a larger gain $\tilde{\boldsymbol{K}}_k$ and a larger covariance $\tilde{\boldsymbol{P}}_{k+1}^{-}$. In literature, there are some works that claim that,[11,18] increasing the process noise covariance matrix $\tilde{\boldsymbol{Q}}_k$ of the Extended Kalman Filter is conceptually the same as increasing the gain $\boldsymbol{K}_k$ and covariance $\boldsymbol{P}_{k+1}$ in the Extended H_∞ Filter using the performance bound γ amending the element $-\gamma\bar{\boldsymbol{S}}_k\boldsymbol{P}_k$ in $\boldsymbol{K}_k$ and $\boldsymbol{P}_{k+1}$.

Before analyzing the filter performance, it is important to analyze their convergence done through configuration of residual represented by the Eq. (30). See Figure 4

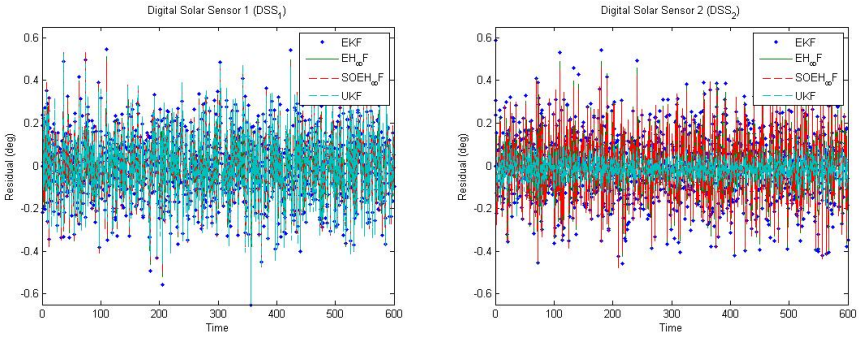

Figure 4: Residuals of the two DSS on board the CBERS-2 satellite

Figure 4 presented the residuals of the two Digital Solar Sensor (DSS), by the estimation methods EKF, EH_∞F, SOEH_∞F and the UKF.

For better visualization of the residuals, in the Fig. 5 below shows the residual frequency for each of the filters in the analysis, presenting characteristics make a Gaussian.

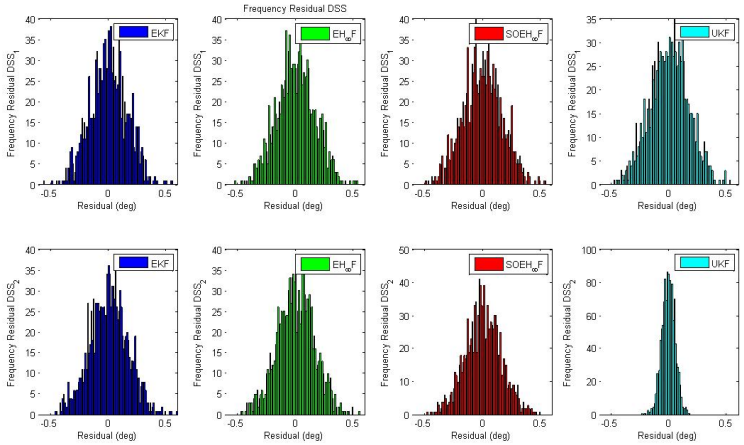

Figure 5: Frequency Residuals of the two DSS on board the CBERS-2 satellite

It is said that a Filter is converging when your residual is close to zero average and it happens with the results presented in Table 1 that shows the average value and the standard deviation of the DSS residuals for each of the filters presented in Figure (5)

Table 1: Mean and standard deviation statistics of the DSS Residuals

	EKF	EH_∞F	SOEH_∞F	UKF
DSS$_1$ Res.(deg)	-0.002 ± 0.160	-0.003 ± 0.163	-0.002 ± 0.165	0.042 ± 1.000
DSS$_2$ Res.(deg)	$-2.6 * 10^{-4} \pm 0.165$	$6.4 * 10^{-5} \pm 0.161$	$-5.4 * 10^{-5} \pm 0.157$	-0.006 ± 1.132

The standard deviation of the DSS Residuals is calculated by Eq (60).

$$\sigma = \sqrt{\frac{1}{K}\sum_{k=1}^{K}(\tilde{\boldsymbol{y}}_k - \bar{\boldsymbol{y}})^2} \tag{60}$$

where $\bar{\boldsymbol{y}} = \frac{1}{K}\sum_{k=1}^{K}\tilde{\boldsymbol{y}}_k$ and K the total number of estimation.

The average results for the DSS_1 Residual are similar for the EKF, EH_∞F, SOEH_∞F and UKF, but the average results for the the DSS_2 Residual presented better result for the H_∞ Filtering, although visually the UKF shows narrowing around the mean zero, but the average value is displaced.

The following, in Figure 6 presented the residuals of the two Infrared Earth Sensor (IRES), for the estimation methods SOEH_∞F, the EH_∞F and the EKF.

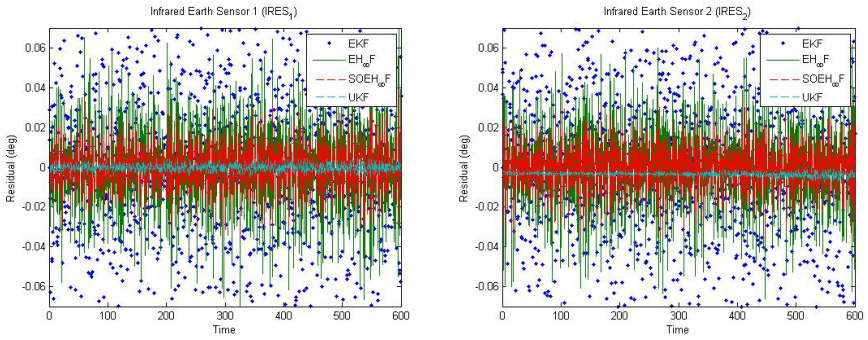

Figure 6: Residuals of the two DSS on board the CBERS-2 satellite

Figure 7 presented the residual frequency of the two Infrared Earth Sensor (IRES), for the estimation methods studied.

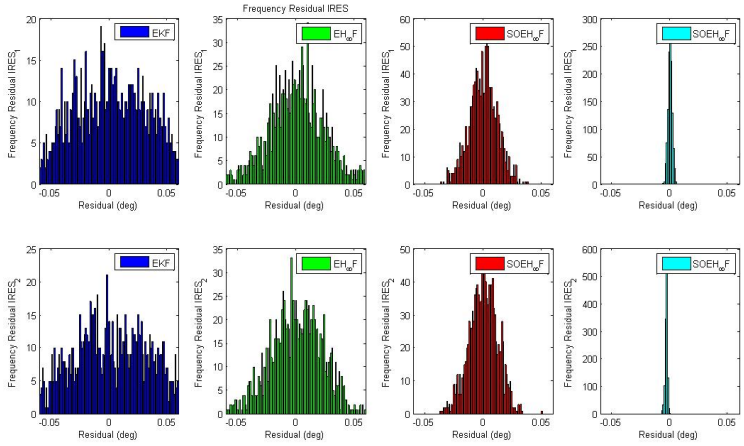

Figure 7: Frequency Residuals of the two DSS on board the CBERS-2 satellite

Here, one can clearly see that, in UKF the residuals converge faster than in SOEH_∞F, EH_∞F and EKF. Results observed by narrowing of Gaussian, see Figure 7. This fact will result in greater accuracy in the state estimation.

The Table 2 shows the average value and the standard deviation of the IRES residuals for each of the filters presented in Fig. (7)

Table 2: Mean and standard deviation statistics of the IRES Residuals

	EKF	EH_∞F	SOEH_∞F	UKF
IRES$_1$ Res.(deg)	$-1.3 * 10^{-4} \pm 0.043$	$-3.4 * 10^{-5} \pm 0.023$	$-2.4 * 10^{-5} \pm 0.012$	0.002 ± 0.110
IRES$_2$ Res.(deg)	$1.5 * 10^{-4} \pm 0.041$	$4.3 * 10^{-5} \pm 0.022$	$7.5 * 10^{-5} \pm 0.012$	0.006 ± 0.165

By the Table 2 all the filters is converging, and the mean the SOEH_∞F present better result for the IRES$_1$ Residual and for the IRES$_2$ Residual, when compared with the EKF, EH_∞F and UKF. Again, although visually the UKF shows narrowing around the mean zero, but the average value is displaced.

To analyze the accuracy of the filters studied, it is presented, in Fig. 8, the error attitude estimation for the methods studied.

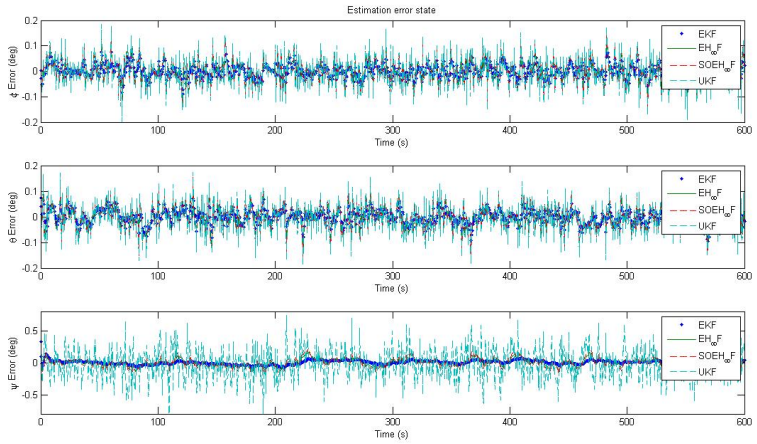

Figure 8: Error attitude estimation

Table 3 shows the average value and the standard deviation of the error attitude estimation presented in Figure (8)

Table 3: Mean and standard deviation statistics of the error attitude estimation

	EKF	EH_∞F	SOEH_∞F	UKF
ϕ Error(deg)	$8.4 * 10^{-4} \pm 0.024$	$9.4 * 10^{-4} \pm 0.041$	$9.5 * 10^{-4} \pm 0.049$	$2.6 * 10^{-4} \pm 0.060$
θ Error(deg)	$-8.8 * 10^{-4} \pm 0.025$	$-9.3 * 10^{-4} \pm 0.040$	$-9.5 * 10^{-4} \pm 0.047$	-0.004 ± 0.057
ψ Error(deg)	0.006 ± 0.032	0.005 ± 0.056	0.005 ± 0.071	-0.005 ± 0.281

With a small change, the standard deviation of the error state estimation is calculated by Eq. (61)

$$\sigma = \sqrt{\frac{1}{K}\sum_{k=1}^{K}(\tilde{\boldsymbol{x}}_k - \bar{\boldsymbol{x}})^2} \tag{61}$$

where $\tilde{\boldsymbol{x}}_k = \hat{\boldsymbol{x}}_k - \boldsymbol{x}_k$, $\bar{\boldsymbol{x}} = \frac{1}{K}\sum_{k=1}^{K}\tilde{\boldsymbol{x}}_k$ and K the total number of estimation.

Analyzing the Table 3 it can be seen that, the average results for the error attitude estimation are basically the same, with a little better in the SOEH_∞F for the θ Error when compared with the EKF, EH_∞F and UKF.

The following, in Figure 9 presented the error bias estimation for the methods studied.

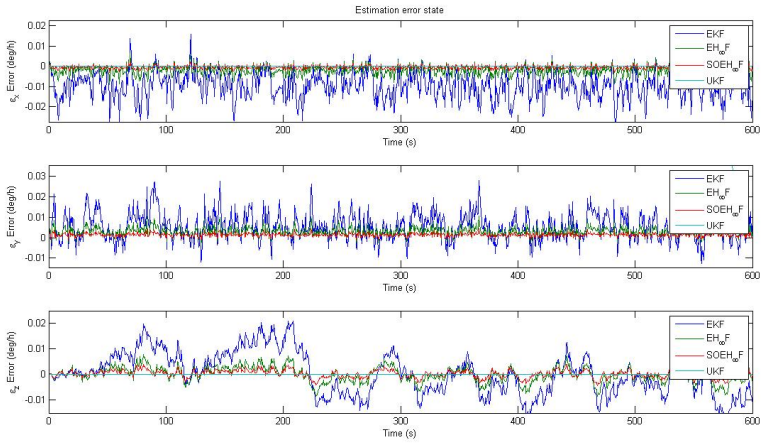

Figure 9: Error gyros bias estimation

Table 4 shows the average value and the standard deviation of the error bias estimation presented in Fig. (9)

Table 4: Mean and standard deviation statistics of the IRES Residuals

	EKF	EH_∞F	SOEH_∞F	UKF
ε_x Error(deg/h)	-0.009 ± 0.006	-0.002 ± 0.002	$-4.4 * 10^{-4} \pm 8.0 * 10^{-4}$	$9.8 * 10^{-4} \pm 1.0 * 10^{-5}$
ε_y Error(deg/h)	0.006 ± 0.006	0.003 ± 0.002	$0.001 \pm 8.4 * 10^{-4}$	0.422 ± 0.191
ε_z Error(deg/h)	$2.8 * 10^{-4} \pm 0.008$	$1.2 * 10^{-4} \pm 0.003$	$2.8 * 10^{-4} \pm 0.001$	$1.3 * 10^{-4} \pm 1.1 * 10^{-5}$

Finally, in the Table 4 is clear that the UKF presents better results for the average of the ε_x Error and the ε_y Error, but for the ε_y Error the SOEH_∞F have better accuracy. Then, the H_∞ filtering and UKF shows superior results in accuracy compared with the EKF, *i.e.*, the attitude estimation and the gyros calibration is much better when accomplished by H_∞ filtering or UKF.

However, this high accuracy comes with a larger processing time, as can be checked in Table 5

The average CPU time was increasing in proportion to the EKF being replaced by the EH_∞F, SOEH_∞F and UKF. On the avarage, the EH_∞F, the SOEH_∞F and the UKF are 0.44s,

Table 5: Comparing processing time cost

	EKF	EH_∞F	SOEH_∞F	UKF
Average CPU time	$1.4201s$	$1.8654s$	$3.4434s$	$3.2713s$

2.02s and 1.85s slower than EKF, respectively. For the SOEH_∞F the result appears due to the large equationing and the second-order derivation, necessary in the filter to be processed and for the UKF the results appears due to the cloud of the sigma-points necessary for the development filter.

7 Conclusions

The usage of real data from on board attitude sensors, poses difficulties like mismodelling, mismatch of sizes, misalignments, unforeseen systematic errors and post-launch calibration errors. However, it is observed that the attitude estimated by the SOEH_∞F and UKF are in close agreement with the results in previous works[16,17] which used the EKF for attitude estimation.

Regarding the robustness of the estimation method SOEH_∞F, it was noted that the results are similar with the reference EKF but the gyros bias covariance by the SOEH_∞F provides results supposedly more accurate for gyros calibration.

According to the theory, the weighting matrices $\boldsymbol{Q}_k$, $\boldsymbol{R}_k$ and $\boldsymbol{S}_k$ in SOEH_∞F are symmetric positive definite matrices which can be designed by the user without requiring them to be diagonal, but the noise covariance matrices $\tilde{\boldsymbol{Q}}_k$ and $\tilde{\boldsymbol{R}}_k$ in EKF are normally set to be diagonal. However, different weighting matrices result in different performance.[18]

It is noted that, the SOEH_∞F can be more robust to the unmodeled noise than the EKF when the weighting matrices $\boldsymbol{Q}_k$ and $\boldsymbol{R}_k$ are the same to the covariance matrices $\tilde{\boldsymbol{Q}}_k$ and $\tilde{\boldsymbol{R}}_k$ of the EKF. The SOEH_∞F is a worst-case filter in the sense that it assumes that the process and measurements noises, $\boldsymbol{w}_k$ and $\boldsymbol{v}_k$ respectively, and the initial condition $\boldsymbol{x}_0$ will be chosen by nature to maximize the cost function. Comparing these filters, we can infer that the SOEH_∞F is simply a robust version of the EKF.

In general terms, for nonlinear system, the Kalman filtering can be used for state estimation, but the UKF may give better results at the price of additional computational effort because the UKF transform a set of points via known nonlinear equations and combines the results to estimate the mean and covariance of the state.

Finally, it can be concluded that the algorithm of the SOEH_∞F and UKF converges, providing a kinematic attitude solution besides estimating biases (gyro drifts) with superior accuracy as compared with the EKF.

ACKNOWLEDGEMENTS

The authors would like to thank the financial support received by CAPES, FAPESP 2012/ 21023-6, CNPQ 303119/ 2010-1, and the partial support from project SIA-DCTA-INPE under contract FINEP 0.1.06.1177.03

Bibliography

[1] J. L. Crassidis and J. L. Junkins, *Optimal Estimation of Dynamic Systems*. New York: Chapman and Hall/CRC Applied Mathematics and Nonlinear Science, 2011.

[2] V. Carrara, "An open source satellite attitude and orbit simulator toolbox for Matlab," *Proceedings...*, Natal, INTERNATIONAL SYMPOSIUM ON DYNAMIC PROBLEMS OF MECHANICS, 17, ABCM, 2015. *Disponível em:* http://mtc-m21b.sid.inpe.br/rep/sid.inpe.br/mtc-m21b/2015/04.07.13.24?. *Acesso em:*: 16 fev. 2016.

[3] E. J. Lefferts, F. L. Markley, and M. D. Shuster, "Kalman filtering for spacecraft attitude estimation," *Journal of Guidance*, Vol. 5, No. 5, 1982, pp. 417 – 429.

[4] J. L. Crassidis, F. L. Markley, and Y. Cheng, "Survey of nonlinear attitude estimation methods," *Journal of Guidance, Control and Dynamics*, Vol. 30, No. 1, 2007, pp. 12 – 28.

[5] K. Shojaie, K. Ahmadi, and A. M. Shahri, "Effects of iteration in Kalman Filters family for improvement of estimation accuracy in simultaneous localization and mapping," *Proceedings...*, Zurich, IEEE/ASME International Conference on Advanced Intelligent Mechatronics, IEEE/ASME, 2007, pp. 1 – 6.

[6] R. V. Garcia, H. K. Kuga, and M. C. Zanardi, "Using extended Kalman filter and least squares method for spacecraft attitude estimation," *Mathematics in Engineering, Science and Aerospace*, Vol. 2, No. 4, 2011, pp. 445–453.

[7] U. Shaked and N. Berman, "H_∞ Nonlinear Filtering of Discrete-Time Processes," *IEEE Transactions on Signal Processing*, Vol. 43, 1995, pp. 2205 – 2209.

[8] R. Banavar, "A game theoretic approach to linear dynamics estimation," 1992.

[9] X. Shen, "Discrete H_∞ filter design with application to speech enhancement," *Proceedings...*, Detroit, IEEE International Conference on Acoustics, Speech and Signal Processing, IEEE, 1995, pp. 1504 – 1507.

[10] X. Shen and L. Deng, "Game theory approach to H_∞ discrete filter design," *IEEE Transactions on Signal Processing*, 1997, pp. 1092 – 1094.

[11] J. S. Hu and C. H. Yang, "Second-Order Extended H_∞ Filter for Nonlinear Discrete-Time Systems Using Quadratic Error Matrix Approximation," *IEEE Transactions on Signal Processing*, Vol. 59, No. 7, 2011, pp. 3110 – 3119.

[12] M. D. Shuster, "A Survey of Attitude Representations," *Journal of Astronautical Sciences*, Vol. 41, No. 4, 1993, pp. 439 – 517.

[13] J. R. Wertz, *Spacecraft attitude determination and control*. Dordrecht, Holanda: D. Reidel,

1978.

[14] J. L. Crassidis and F. L. Markley, "Unscented filtering for spacecraft attitude estimation," *Journal of Guidance, Control and Dynamics*, Vol. 26, No. 4, 2003, pp. 536 – 542.

[15] H. Fuming and H. K. Kuga, "CBERS simulator mathematical models," *CBTT Project, CBTT/ 2000/ MM/ 001*, 1999.

[16] R. V. Garcia, H. K. Kuga, and M. C. Zanardi, "Unscented Kalman filter applied to the spacecraft attitude estimation with euler angles," *Mathematical Problems in Engineering*, Vol. 2012, 2012, pp. 1–12.

[17] R. V. Garcia, H. K. Kuga, and M. C. Zanardi, "Unscented Kalman filter for spacecraft attitude estimation using quaternions and euler angles," *Proceedings...*, São José dos Campos, International Symposium on Space Flight Dynamics, 22, AAB, 2011.

[18] D. Simon, *Optimal State Estimation*. New York: Wiley, 2006.

[19] W. R. Silva, H. K. Kuga, and M. C. Zanardi, "Application fo the Extended H_∞ Filter for Attitude Determination and Gyro Calibration," *Advances in the Astronautical Sciences*, 2014, pp. 1501 – 1515.

[20] S. J. Julier and J. K. Uhlmann, "A new extension of the Kalman Filter for nonlinear systems," *Signal Processing, Sensor Fusion, and Target Recognition*, Vol. 3068, 1997, pp. 182 – 193.